Journal of Alloys and Compounds 509 (2011) 2445–2449

Contents lists available at ScienceDirect

Journal of Alloys and Compounds

journal homepage: www.elsevier.com/locate/jallcom

Solution combustion synthesis and characterization of lead-free piezoelectric sodium niobate ($NaNbO_3$) powders

Nopsiri Chaiyo[a,b], Rangson Muanghlua[c], Surasak Niemcharoen[c],
Banjong Boonchom[d], Naratip Vittayakorn[a,b,e,*]

[a] Electroceramic Research Laboratory, College of KMITL Nanotechnology, King Mongkut's Institute of Technology Ladkrabang, Bangkok 10520, Thailand
[b] ThEP Center, CHE, 328 Si Ayutthaya Rd., Bangkok 10400, Thailand
[c] Department of Electronics, Faculty of Engineering, King Mongkut's Institute of Technology Ladkrabang, Bangkok 10520, Thailand
[d] King Mongkut's Institute of Technology Ladkrabang, Chumphon Campus, 17/1 M. 6 Pha Thiew District, Chumphon 86160, Thailand
[e] Department of Chemistry, Faculty of Science, King Mongkut's Institute of Technology Ladkrabang, Bangkok 10520, Thailand

ARTICLE INFO

Article history:
Received 20 July 2010
Received in revised form 27 October 2010
Accepted 8 November 2010
Available online 13 November 2010

Keywords:
Sodium niobate
Modified solid state reaction

ABSTRACT

Nano-crystalline sodium niobate ($NaNbO_3$) powder was synthesized by the solution combustion synthesis of sodium nitrate ($NaNO_3$) and Nb_2O_5 using glycine as the fuel. The chemical reaction, nucleation mechanisms and influence of the fuel-to-oxidizer ratio to phase formation were studied. The precursor and product powders were characterized, using thermo gravimetric analysis (TGA), differential thermal analysis (DTA), the X-ray diffraction technique (XRD), scanning electron microscope (SEM) and Fourier transform infrared (FTIR) spectroscopy. As-prepared powder possesses an orthorhombic crystal structure with an X-ray diffraction pattern that could be matched with the perovskite, $NaNbO_3$ JCPDS no. 82-0606. Perovskite $NaNbO_3$ phase, with a mean crystalline size (calculated by X-ray line broadening) ranging from 44.51 ± 11.99 nm (ratio of 0.7) to 26.11 ± 13.69 nm (ratio of 2.0) was obtained. The SEM image shows polyhedral-shaped powder with a mean particle size of 137 ± 52 nm and 226 ± 46 nm for as-prepared and calcined powder, respectively.

1. Introduction

Sodium niobate ($NaNbO_3$) is a perovskite with an inorganic complex oxide and the empirical formula, ABO_3. It is among the candidates for lead-free substances that avoid toxicity of lead-based piezoelectric materials (e.g. PZT [1,2]), and is concerned about the environment. $NaNbO_3$ has been studied widely for its unusual structural transition series [3–7]. It has a ferroelectric rhombohedral phase below $-100\,^\circ C$, and is antiferroelectric with orthorhombic symmetry between $-100\,^\circ C$ and $640\,^\circ C$ [4]. Finally, it possesses cubic paraelectric above $640\,^\circ C$ [5], and in addition, its antiferroelectric, perovskite-type nature can transform into a ferroelectric one by chemical doping, i.e. K^+ [6,7] and Li^+ [8].

Generally, alkali niobate powders are synthesized by conventional solid state reaction, where alkali metal carbonate or oxide compound of starting materials are heated at high temperature ($800\,^\circ C$ or above) for a long duration [8,9]. High calcination temperature can cause volatilization of alkali metal, thus causing this classical method difficulty in achieving a homogeneous mixture of the component [8–10]. Powder agglomeration can occur during heating, which could affect properties such as low surface area and low sinterability [10]. Thus, this method does not always allow for the production of dense, homogeneous single phase ceramics. Therefore, development of alternative methods that can produce powder with high sinterability and controlled stoichiometric composition is necessary. In recent years, ultra fine ceramic powder, which is synthesized using mechanochemical synthesis [11], polymeric precursors [12], and hydrothermal and polymerized complex methods [13], has been described in the literature to enable production of desired compositions. While synthesizing powder rapidly, with the desired composition, high porosity and high sinterability remains a challenge, combustion synthesis (CS) has been found as a potential solution for this problem.

Combustion synthesis (CS) or self-propagating high temperature synthesis (SHS) is an effective, low-cost method for producing various industrially useful materials. It has been introduced as a quick, straightforward preparation process for producing homogeneous, very fine, crystalline and unagglomerated multicomponent oxide ceramic powders, without intermediate decomposition and/or calcination steps [14,15]. The combustion synthesis technique begins with a mixture of easily oxidized reactants (such as nitrates) and a suitable organic fuel (such as urea [16], tartalic acid

---

* Corresponding author at: Department of Chemistry, Faculty of Science, King Mongkut's Institute of Technology Ladkrabang, Bangkok 10520, Thailand.
Fax: +66 2 326 4415.
E-mail address: naratipcmu@yahoo.com (N. Vittayakorn).

0925-8388/$ – see front matter © 2010 Elsevier B.V. All rights reserved.
doi:10.1016/j.jallcom.2010.11.043

[17], alanine [18], glycine [19], etc.), which acts as a reducing agent. The mixture is then heated until it ignites, which is when the temperature of rapid exothermal chemical reaction commences, and a self-sustaining combustion reaction starts. This highly exothermic reaction produces a high temperature and duration long enough for the synthesis to occur, even in the absence of an external heating source [20]. Ultrafine nano-sized powder also can be prepared by releasing a large amount of gas from the system. This process results in a dry, fluffy, crystalline, unagglomerated and fine oxide powder. Metal nitrate was found to be the salt preferred, due to its water solubility, and homogeneous solution could be achieved easily by melting at a low temperature [16].

However, it was reported that an exothermic redox reaction (oxidation and reduction reaction taking place simultaneously) could be initiated only when the oxidizer and fuel are mixed intimately in a fixed proportion. The basis of the combustion synthesis process derives from the thermochemical concepts used in propellant chemistry [21,22]. The method consists of establishing a simple valency balance, irrespective of whether the elements are present in the oxidizer or fuel components of the mixture, and then calculating the stoichiometric composition of the starting mixture, which is equivalent to the release of maximum energy. The assumed valencies, which are presented as usual products of the combustion reaction, consist of CO_2, H_2O and N_2. Therefore, carbon and hydrogen are considered as reducing elements with the corresponding valencies of +4 and +1, whereas oxygen is thought to be an oxidizing agent with a valency of −2, and nitrogen a valency of 0. To extrapolate the concept of combustion synthesis of ceramic oxide means considering metals as reducing agents with their valencies in the corresponding oxide or nitrate, i.e. +2 for magnesium (oxide), +3 for cerium (nitrate) and +4 for cerium (oxide). In the case of multiple valence elements, the final product is used for calculation.

The elemental stoichiometric coefficient, φ, which is the ratio between the total valencies of fuel (glycine; NH_2CH_2COOH) and that of the oxidizer (sodium nitrate), can be calculated following the method proposed by Jain et al. [21]:

$$\varphi = \frac{n(0_{(N)} + 2\times 1_{(H)} + 4_{(C)} + 2\times 1_{(H)} + 4_{(C)} - 2_{(O)} - 2_{(O)} + 1_{(H)})}{1_{(Na)} + 0_{(N)} + 3\times -2_{(O)}} \quad (1)$$

where n is the mole of glycine. According to the propellant chemistry for stoichiometric redox reaction between fuel and an oxidizer, the φ ratio should be united (stoichiometric). A $\varphi < 1$ means oxidant-rich condition and $\varphi > 1$ means fuel-rich condition. To satisfy the principle in the present system, the sodium nitrate (oxidizing valency = 5−) to glycine (reducing valency = 9+) molar ratio was found to be 1:0.56. The comprehensive reaction that formed $NaNbO_3$ can be written as:

$$36NaNO_3 + 18Nb_2O_5 + 20NH_2CH_2COOH \rightarrow 36NaNbO_3 + 50H_2O + 28N_2 + 40CO_2 \quad (2)$$

It should be noted that various fuel-to-oxidizer ratios should be carried out for investigating and comparing the effect of fuel-rich/fuel-lean mixtures on the synthesis of sodium niobate powder. In this study, sodium niobate powder was synthesized via the combustion synthesis technique for the first time. This process used sodium nitrate and niobium pentoxide as starting materials, and glycine was used as fuel. The different fuel-to-oxidizer molar ratios such as fuel-deficient (<0.56), equivalent stoichiometric (0.56) and fuel-rich (>0.56) condition were applied.

2. Experimental procedure

For the combustion synthesis of perovskite sodium niobate powder, AR grade sodium nitrate ($NaNO_3$ 99.5%) and niobium pentoxide (Nb_2O_5 99.95%) were used as the oxidizer, and glycine (NH_2CH_2COOH 99.7%) as fuel. The appropriate amount of starting materials was weighed, mixed with de-ionized water in a glass beaker and stirred regularly for 30 min. The fuel (glycine) was then added and the mixture stirred for 30 min. After that, the solution precursor was boiled on a hotplate and then evaporated. Once the solution had thickened and begun to dry, the ignition took place when the temperature rapidly increased, which resulted in self-sustaining combustion with rapid evolution of a large volume of gas products, and formation of voluminous powder. For investigating thermal behavior of the precursor, the mixture of starting material was determined using thermo gravimetric analysis (TGA) and differential thermal analysis (DTA). The X-ray diffraction (XRD, Advance D8) technique was carried out on the combustion synthesized powder, using Ni-filtered CuK$_\alpha$ radiation for phase identification and mean crystalline size estimation. The final powder product was characterized by using the Fourier transform infrared (FTIR) technique and scanning electron microscope (SEM, Hitachi S4700).

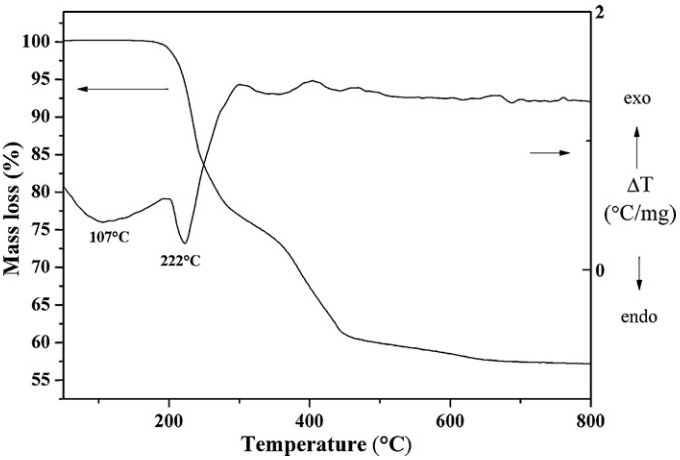

Fig. 1. TG-DTA curves of the precursor mixed in the stoichiometric proportion of $NaNbO_3$.

3. Results and discussion

Fig. 1 shows the TG/DTA plots of the stoichiometric precursor for $NaNbO_3$ powder synthesis. From observations of the TGA curve, there appeared to be three-stages of weight loss from room temperature to 800 °C. The definition of initial temperature (T_{in}) is when the sample weight starts changing rapidly during the chemical reaction [23]. As the precursor was heated, a significant weight loss was observed as the temperature reached 170 °C, indicating that the T_{in} was around this heat. The weight loss did not stop until the temperature reached 480 °C. It was indicated clearly that this reaction belongs to a multi-stage reaction. The overall weight loss was found to be about 40%, which is close to the theoretical value of 36.87% that corresponds to the release of 50 mol H_2O, 28 mol N_2 and 40 mol CO_2 related to Eq. (2). This outcome supported our conception that a hotplate can be used as a heating source because it is capable of initiating the combustion reaction at a temperature as low as that of the T_{in}.

The evolution XRD pattern of the combustion synthesized ceramic powder, with the fuel-to-oxidizer molar ratio, is illustrated in Fig. 2. The fuel-deficient (0.5) and equivalent stoichiometric ratio (0.56), were found (according to experimental observation) to have no ignition and combustion reaction in those compositions. Their XRD patterns correlated to detection results of the diffraction peaks of Nb_2O_5 (●) (JCPDS file no. 30-0873) and $NaNO_3$ (■) (JCPDS file no. 85-0859) starting materials, with no evidence of perovskite $NaNbO_3$ phase found. Although the equivalent stoichiometric ratio (0.56) was calculated for maximum energy release, auto-ignition did not occur in this study. This could indicate that oxygen deficiency in the system and its environment might lead to combustion reaction and fail to follow the theory. The fuel-to-oxidizer molar ratio was increased by using the fuel-rich condition (>0.56), which was found to produce the perovskite $NaNbO_3$ ceramic powder, due to its diffraction peaks being detected for all different fuel contents

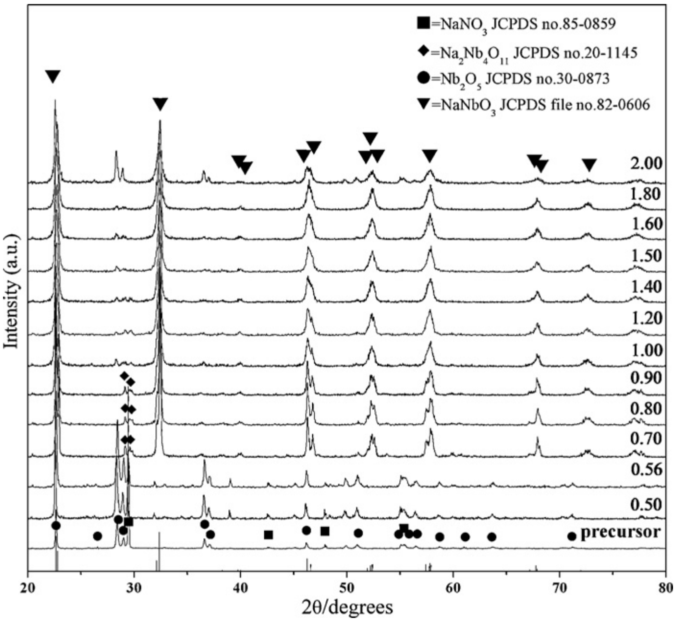

Fig. 2. X-ray diffraction patterns of $NaNbO_3$ powder obtained from various fuel-to-oxidant molar ratios.

(fuel-to-oxidizer molar ratio ranging from 0.7 to 2.0). This $NaNbO_3$ phase (▼) was consistent with JCPDS file no. 82-0606, which corresponded to an orthorhombic structure with the space group, $P2_1ma$ (26). For a fuel-rich condition (fuel-to-oxidizer molar ratio of 0.7, 0.8 and 0.9), the $NaNbO_3$ phase (▼) was detected with the accompanying pyrochlore phase of $Na_2Nb_4O_{11}$ (◆), which matched JCPDS file no. 20-1145. No evidence of unreacted Nb_2O_5 and/or $NaNO_3$ diffraction peak was found. As fuel content increased from the fuel-to-oxidizer molar ratio of 1.0–2.0, unreacted Nb_2O_5 (●) (JCPDS file no. 30-0873) was found together with a majority of $NaNbO_3$ diffraction peaks. From the reflection peak, the average crystalline size (D) of $NaNbO_3$ powders was considered as a function of fuel content by using X-ray line broadening through Scherrer's equation [24]:

$$D = \frac{k\lambda}{\beta \cos\theta_B} \tag{3}$$

where D is the average crystalline size, k a constant taken as 0.89, λ the wavelength of X-ray radiation, β the full width at half maximum (FWHM) and θ_B the diffraction angle. The consequent values are reported in Table 1. As the fuel content increased, the average crystalline size (D) was found to decreased from 44.51 ± 11.99 nm (ratio of 0.7) to 26.11 ± 13.69 nm (ratio of 2.0). This suggested that elevated fuel content could lead to the production of a smaller crystalline size (related to a small particle size) of powder. Nevertheless, as a consequence of additional cost and more carbon residual, an extremely high fuel-to-oxidizer molar ratio (fuel-rich ratio) did not always result in the desired production of powder [25].

Therefore, from findings on the fine nucleation condition of monophasic $NaNbO_3$ phase, the fuel-to-oxidizer molar ratio of 1.0 was selected to investigate the effect of calcination temperature. From this ratio, the volume fraction of the perovskite phase formation (%perovskite) of as-prepared powder was found to be as high as 93%. This relative value was considered by approximately calculating the ratio of the main X-ray peak intensities of $NaNbO_3$ and Nb_2O_5 phases [26], according to the following equation; $\%\ \text{perovskite} = (I_{\text{perovskite}}/(I_{\text{perovskite}} + I_{\text{Nb}_2}O_5)) \times 100$. Thus, the as-prepared powder was calcined at different temperatures for 4 h with a heating/cooling rate of 20 °C/min. The X-ray diffraction (XRD) patterns of sodium niobate ($NaNbO_3$) powder, calcined for 4 h at different temperatures, are illustrated in Fig. 3. As the XRD pattern of as-prepared powder was composed of a slight Nb_2O_5 (●) (JCPDS file no. 30-0873) phase, the intensity of that phase was found to decrease with increasing calcination temperature. The diffraction peak corresponded to the Nb_2O_5, which disappeared after calcination at 400 °C for 4 h, whereas monophasic perovskite $NaNbO_3$ phase was obtained. This result suggested that the perovskite $NaNbO_3$ powder could be synthesized by using the combustion synthesis process and calcinations at 400 °C for 4 h. This process was found to be a simple, rapid and cost-effective method when compared with the traditional solid-state reaction, which takes longer time and requires higher temperature [8,9]. In addition, the mean crystalline size (D), which is reported in Table 1, was not significantly varied between as-prepared powder (29.28 ± 5.29 nm) and increasing calcination temperatures of up to 400 °C (27.84 ± 7.12 nm). It can be suggested that calcina-

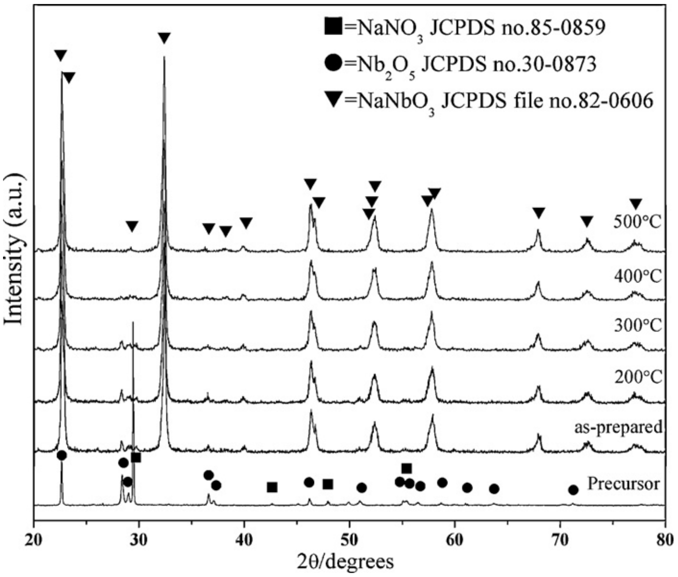

Fig. 3. X-ray diffraction patterns of $NaNbO_3$ powder (obtained from the fuel-to-oxidant molar ratio of 1.0) calcined at various temperatures for 4 h with a heating/cooling rate of 20 °C/min.

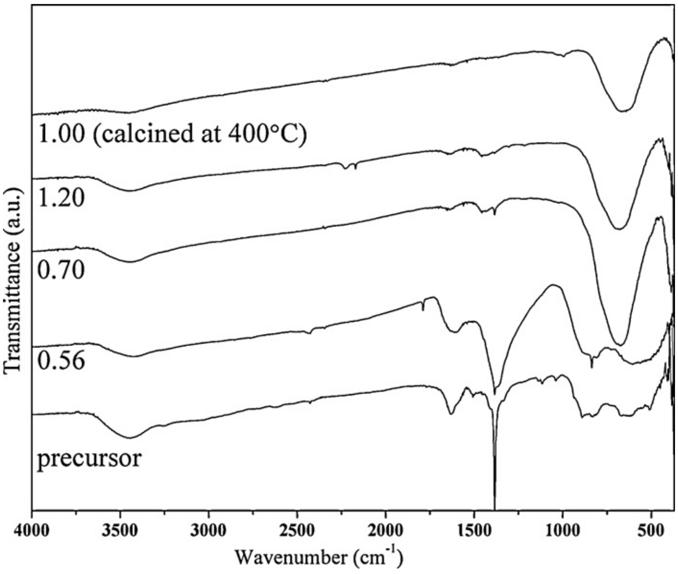

Fig. 4. FT-IR spectra of the precursor mixed in the stoichiometric proportion of $NaNbO_3$ powder obtained from various fuel-to-oxidant molar ratios and after the calcination step.

Table 1
Mean crystalline size, *D*, of $NaNbO_3$ powder obtained from various fuel-to-oxidant molar ratios.

	Fuel-to-oxidant molar ratios								
	0.7	0.8	0.9	1.0	1.2	1.4	1.6	1.8	2.0
As-prepared	44.51 ± 11.99	42.59 ± 11.54	37.31 ± 8.54	29.09 ± 5.29	27.45 ± 5.86	26.29 ± 5.97	24.40 ± 4.92	23.79 ± 5.52	26.12 ± 13.69

	Calcination temperature (°C)							
	200 °C	300 °C	400 °C	500 °C	600 °C	700 °C	800 °C	900 °C
Calcined powder	29.95 ± 4.51	31.51 ± 4.02	27.84 ± 7.12	30 ± 82 ± 5.43	38.84 ± 8.09	60.72 ± 8.09	70.87 ± 9.22	85.27 ± 15.65

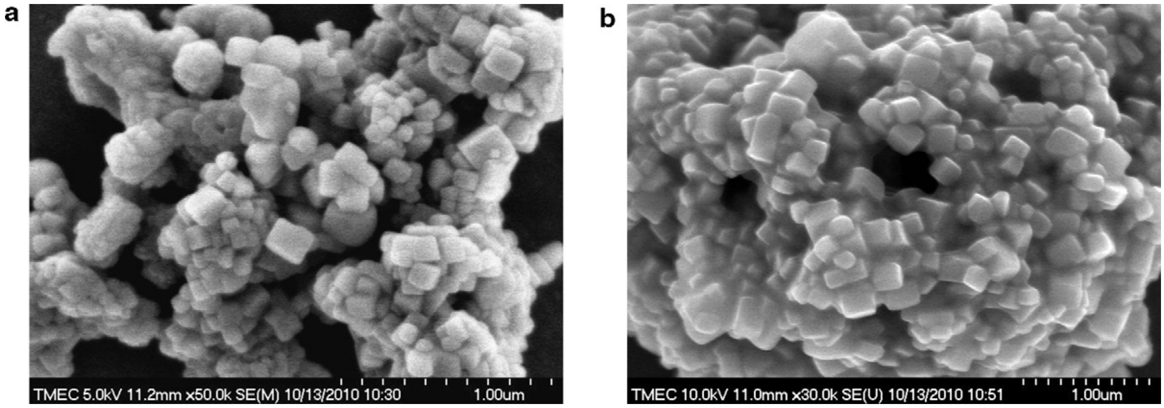

Fig. 5. SEM micrograph showing as-prepared $NaNbO_3$ powder synthesized using the fuel-to-oxidant molar ratio of 1.0 (a) and powder calcined at 400 °C for 4 h (b).

tions at this low temperature also produced a lower crystalline size when compared with the traditional solid state reaction method.

Fig. 4 shows the FT-IR spectroscopic studies of the crystalline $NaNbO_3$ obtained after combustion synthesis, its precursor without heat treatment and powder calcined at 400 °C for 4 h. For all powder, an IR band of around 3400 cm^{-1} was assigned to O–H asymmetric stretching (ν_3) [27], and on observation, it related to the moisture content of KBr. Regarding the precursor of $NaNbO_3$ powders without heat treatment, and as-prepared powder with a stoichiometric ratio (0.56), the IR spectrum indicated peaking of the characteristic band at ~1612, ~1385 and ~890 cm^{-1}, which corresponded to the anti-symmetric carboxyl group stretching vibration, anti-symmetry $NO_3{}^{-1}$ stretching and bending vibration, respectively [28]. This result proved existence of the carboxyl and $NO_3{}^{-1}$ group (belonging to the starting material) in those samples. With regard to fuel-rich ratios (0.7 and 1.2), the new broad absorption bands appeared after combustion at a low wave number of ~673 cm^{-1}, suggesting that the Nb–O bond formation did occur. This Nb–O bond was believed to be the vibration (ν_3) mode in the corner-shared NbO_6 octahedron, according to reported IR spectra of niobate glass ceramics [28]. This result led to the assumption that the perovskite $NaNbO_3$ phase was synthesized (which correlated to XRD analysis). However, the IR band of anti-symmetric COO^- and that of anti-symmetry $NO_3{}^{-1}$ stretching vibration also were observed. This clearly indicated traces of existent carboxyl group and nitrate in as-prepared $NaNbO_3$ powder, which cannot be detected when using the XRD technique. For powder calcined at 400 °C for 4 h, the spectra band of vibration (ν_3) mode belonging to the Nb–O bond was found without observation of any starting material band. This can indicate that monophasic perovskite $NaNbO_3$ has been synthesized successfully after calcination at a temperature as low as 400 °C for 4 h. Fig. 5 shows an SEM micrograph of the as-prepared $NaNbO_3$ powder using the fuel-to-oxidizer molar ratio of 1.0 (a) and powder calcined at 400 °C for 4 h (b). The powder was found to be polyhedral in shape, with uniform features. No evidence of a different or pyrochlore phase was found, which suggested the homogeneous character of the prepared powder. The average particle size, which can be estimated from micrographs, was found to be 137 ± 52 nm and 226 ± 46 nm for as-prepared and calcined powder, respectively. These particle size values are greater than the average crystalline size calculated from X-ray line broadening because a particle can be formed generally of many crystallites [29–31]. The particle growth for calcined powder seemed to be detected. It can be said that the firing process tends to produce agglomerated particles and grain growth, as reported by other works [32,33].

4. Conclusions

Crystalline $NaNbO_3$ powder, with a volume fraction of the perovskite phase formation (% perovskite) as high as 93%, was synthesized directly via the solution combustion process using $NaNO_3$, Nb_2O_5 and glycine. Monophasic perovskite $NaNbO_3$ powder was obtained after calcination at 400 °C for 4 h. The fuel-to-oxidizer molar ratio was found to affect the combustion reaction and character of the powder obtained. The average crystalline size (*D*) was found to decrease from 44.51 ± 11.99 nm (ratio of 0.7) to 26.11 ± 13.69 nm (ratio of 2.0). This method is a simple, rapid, cost- and time-saving way of synthesizing stoichiometric, homogeneous and fine $NaNbO_3$ powder with a low calcination temperature. The powder obtained was found to be a uniform soft agglomerated particle.

Acknowledgements

This work was supported by the Thailand Research Fund (TRF), Thailand Graduate Institute of Science and Technology (TGIST), King Mongkut's Institute of Technology Ladkrabang Research (KMITL Research), and the National Nanotechnology Center (NANOTEC) NSTDA, Ministry of Science and Technology, Thailand through its "Center of Excellence Network" Program.

References

[1] B. Jaffe, W.R. Cook Jr., H. Jaffe, Piezoelectric Ceramics, Academic Press, New York, 1971.
[2] B. Jaffe, R.S. Roth, S. Marzullo, J. Appl. Phys. 25 (1954) 809–810.
[3] N. Chaiyo, B. Boonchom, N. Vittayakorn, J. Mater. Sci. 45 (2010) 1443.
[4] H.D. Megaw, Ferroelectrics 7 (1974) 87–89.
[5] L.E. Cross, B. Nicholson, J. Phil. Magn. Ser. 46 (1955) 453–466.
[6] G. Shirane, B. Newnham, R. Pepinsky, Phys. Rev. 96 (1954) 581–588.
[7] Y. Shiratori, A. Magrez, C. Pithan, J. Eur. Ceram. Soc. 25 (2005) 2075–2079.
[8] T. Nitta, J. Am. Ceram. Soc. 51 (1968) 626–629.
[9] T. Rojac, O. Masson, R. Guinebretière, M. Kosec, B. Malič, J. Holc, J. Eur. Ceram. Soc. 17 (2007) 2265–2271.
[10] C.C. Hwang, T.Y. Wu, J.S. Tsai, Mater. Sci. Eng. B 111 (2004) 49–56.
[11] T. Rojac, M. Kosec, B. Malič, J. Holc, Mater. Res. Bull. 40 (2005) 341–345.
[12] M.A.L. Nobre, E. Longo, E.R. Leite, J.A. Varela, Mater. Lett. 28 (1996) 215–220.
[13] G. Li, T. Kako, D. Wang, Z. Zou, J. Ye, J. Phys. Chem. 69 (2008) 2487–2491.
[14] K.C. Patil, S.T. Aruna, S. Ekambaram, Curr. Opin. Solid State Mater. Sci. 2 (1997) 158–165.
[15] K.C. Patil, S.T. Aruna, T. Mimani, Curr. Opin. Solid State Mater. Sci. 6 (2002) 507–512.
[16] D.A. Fumo, M.R. Morelli, A.M. Segadães, Mater. Res. Bull. 31 (1996) 1243–1255.
[17] M.A. Raza, I.Z. Rahman, S. Beloshapkin, J. Alloys Compd. 485 (2009) 593–597.
[18] M.W. Raja, S. Mahanty, P. Ghosh, R.N. Basu, H.S. Maiti, Mater. Res. Bull. 42 (2007) 1499–1506.
[19] S.V. Chavan, P.U.M. Sastry, A.K. Tyagi, J. Alloys Compd. 456 (2008) 51–56.
[20] N.P. Bansal, Z. Zhong, J. Power Sources 158 (2006) 148–153.
[21] S.R. Jain, K.C. Adiga, V.R.P. Verneker, Combus. Flame 40 (1981) 71–79.
[22] S.S. Manoharan, K.C. Patil, J. Am. Ceram. Soc. 75 (1992) 1012–1015.
[23] L.A. Chick, L.R. Pederson, G.D. Maupin, J.L. Bates, L.E. Thomas, G.J. Exarthos, Mater. Lett 10 (1990) 6–12.
[24] H.P. Klug, L.E. Alexander, X-ray Diffraction Procedure of Polycrystalline and Amorphous Materials, Jonh Wciley & Sons, New York, 1974.
[25] A. Civera, M. Pavese, G. Saracco, V. Specchia, Catal. Today 83 (2003) 199–211.
[26] G. Feng, H. Rongzi, L. Jiaji, L. Zhen, C. Lihong, T. Changsheng, J. Eur. Ceram. Soc. 29 (2009) 1687–1693.
[27] C. Weifan, L. Fengsheng, L. Leili, L. Yang, J. Rare Earths 24 (2006) 782–787.
[28] S.H Xiao, W.F. Jiang, L.Y. Li, X.J. Li, Mater. Chem. Phys. 106 (2007) 82–87.
[29] M.L. Lavčević, A. Turković, Scripta Mater. 46 (2002) 501–505.
[30] W.-N. Wang, W. Widiyastuti, T. Ogi, I.W. Lenggoro, Chem. Mater. 19 (2007) 1723–1730.
[31] N. Izu, W. Shin, I. Matsubara, N. Murayama, Sens. Actuators B 94 (2003) 222–227.
[32] Y. Terashi, A. Purwanto, W.N. Wang, F. Iskandar, K. Okuyama, J. Eur. Ceram. Soc. 28 (2008) 2573.
[33] R. Wongmaneerung, W. Chaisan, O. Khamman, R. Yimnirun, S. Ananta, Ceram. Int. 34 (2008) 813.